Understanding of Interactions Between Pyrolysis Gases and Liquid Aluminum and Their Impact on Dross Formation

R. Dittrich, B. Friedrich, G. Rombach, J. Steglich, and A. Pichat

Abstract

Organic contaminated aluminum scraps have to be recycled in an economical, effective and ecological way. It is state of the art to remove organic coatings by thermal pre-treatment under reduced oxygen atmosphere, which can be achieved in multi chamber furnaces. If the organic coating is not removed completely during pre-treatment, gasification can continue while the scrap is submerged into the melt. Subsequently, undesirable gas-melt reactions cause an increase of dross formation and a decrease of metal recovery. This work aims to improve the understanding of interactions between pyrolysis gases and liquid aluminum as a scientific basis to reduce oxidation losses. Experiments were performed in a lab-scale furnace with injection of synthetic pyrolysis gases (CO_2, CO, C_xH_y) into molten aluminum. Thermochemical calculations, off-gas and dross structure analysis were performed to support the evaluation of the experimental findings. The paper presents qualitative and quantitative results about the impact of reactive gases on oxidation of aluminum melts and finally derives a mechanism model.

Keywords

Pyrolysis gases • Gas injection • Dross formation

Introduction

Large amounts of organic contaminated scraps have to be recycled in modern salt free furnaces with integrated thermal pre-processing. The main challenge in this process is to find the optimum for high efficiency in de-coating, melt grade as well as energy consumption. Results of thermal pre-treatment of Used Beverage Can (UBC) scraps in an industrial reverberatory multi-chamber shaft furnace have shown that the average residence time is too short to complete the pyrolysis process. This has been based on the typical observation of the non-pyrolysed cores inside the Al-bales [1]. As a consequence of productivity requirements, gasification continues while the bale is being immersed into the melt. Such pyrolytic gaseous products can have long residence time inside the melt, promoting undesired gas-liquid reactions, which leads to a significant dross formation.

The thermal removal of organic contaminants (coatings) on aluminum scrap depends on time, temperature, atmosphere, heat transfer and package density [2]. Pyrolysis products consist of solid char and energy rich gas components, which can be post-combusted in the melting chamber. In Fig. 1 the thermal degradation of coated beverage cans is shown. The thermal decomposition of epoxy resin starts at

R. Dittrich (✉) · B. Friedrich
IME Institute of Process Metallurgy and Metal Recycling, RWTH Aachen University, Intzestr. 3, 52056 Aachen, Germany
e-mail: RDittrich@ime-aachen.de

G. Rombach
Hydro Aluminium Rolled Products GmbH, Georg-Von-Boeselager-Str. 21, 53117 Bonn, Germany

J. Steglich
TRIMET Aluminium SE, Aluminiumallee 1, 45356 Essen, Germany

A. Pichat
Constellium Technology Center, Parc Economique Centr'alp, CS 1002738341 Voreppe cedex, France

A.P. Ratvik (ed.), *Light Metals 2017*, The Minerals, Metals & Materials Series,
DOI 10.1007/978-3-319-51541-0_174

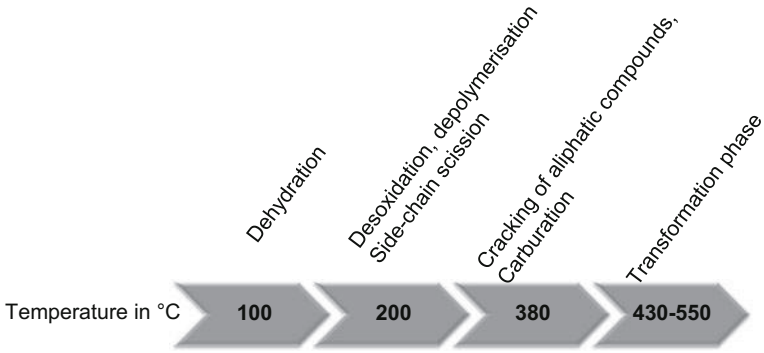

Fig. 1 Thermal decomposition of coatings as a function of temperature [3–5]

200 °C involved by chain scission and stripping of side groups. Small molecules such as acetaldehyde and short chain aliphatic compounds are gasified. With increasing temperature the macromolecular polymers can be cracked depending on its bond-dissociation energy. Typical gaseous pyrolytic products from epoxy resin are aromatic compounds e.g. phenol [3–5].

In the case of the submerged non-pyrolyzed bales in the melt, evolved phenol can be directly decomposed to smaller molecules. Additionally, cyclopentadiene (C_5H_6) and CO are the major intermediate reactions under these conditions [6]. In the transformation phase the solid residues are further split into more stable gases like H_2, CO, CO_2 and CH_4. A further temperature increase to 600 °C has not effects on decomposition [3–5].

Based on the assumption that long-chain carbon hydrogens decompose under heat effect to smaller molecules, the reactivity of four carbon containing gas components (CO_2, CO, CH_4 and C_4H_{10}) with molten aluminum is experimentally investigated in this work. Additionally, oxygen is injected into liquid aluminum to model enclosed air in scrap bales.

Gas—Liquid Reactions

Several research topics focus on the oxidation mechanism of quiescent aluminum melt in long- time tests. During melting of pure aluminum, oxide growth follows three steps. At the beginning a tiny amorphous oxide layer is formed rapidly on the melt surface. Secondly, a phase transformation from amorphous to crystalline γ-Al_2O_3 takes place, which hinders further oxidation. In the third step, breakaway oxidation has been observed, which is caused by a phase transformation from γ-Al_2O_3 to α-Al_2O_3, accompanied by volume change of the oxides. As such, the oxidation rate increases drastically due to the formed cracks in the oxide layer, in which aluminum and oxygen ions may diffuse [7–9].

The dynamic oxidation of liquid aluminum by injection of reactive gases such as CO_2 has been previously studied by Wightman et al. [10]. They have assumed that molten aluminum is oxidized by CO_2 resulting in formation of CO and alumina, as shown in reaction 1. All free energy ΔG° values are obtained by using the software FactSage 6.4 [11].

$$\begin{gathered}\mathrm{Al_{(l)}} + \frac{3}{2}\mathrm{CO_{2_{(g)}}} = \frac{1}{2}\mathrm{Al_2O_{3_{(s)}}} + \frac{3}{2}\mathrm{CO_{(g)}} \\ \Delta G(1023\,\mathrm{K}) = -379\,\mathrm{kJ/mol}\end{gathered} \tag{1}$$

Reaction 1 is controlled by the rate of desorption of CO from aluminum oxide. Reaction 2 describes the interaction between CO and liquid aluminum, which results in formation of carbon and more alumina.

$$\begin{gathered}\mathrm{Al_{(l)}} + \frac{3}{2}\mathrm{CO_{(g)}} = \frac{1}{2}\mathrm{Al_2O_{3_{(s)}}} + \frac{3}{2}\mathrm{C_{(s)}} \\ \Delta G(1023\,\mathrm{K}) = -367\mathrm{kJ/mol}\end{gathered} \tag{2}$$

From the thermochemical aspect, formation of aluminum carbides might occur. However, due to re-oxidation with CO_2, the reaction would lead to more formation of Al_2O_3 and free carbon. See Eqs. 3 and 4.

$$\mathrm{Al_{(l)}} + \frac{3}{4}\mathrm{C_{(s)}} = \frac{1}{4}\mathrm{Al_4C_{3_{(s)}}} \quad \Delta G(1023\,\mathrm{K}) = -43\,\mathrm{kJ/mol} \tag{3}$$

$$\begin{gathered}\frac{1}{4}\mathrm{Al_4C_{3_{(s)}}} + \frac{3}{4}\mathrm{CO_{2_{(g)}}} = \frac{1}{2}\mathrm{Al_2O_{3_{(s)}}} + \frac{3}{2}\mathrm{C_{(s)}} \\ \Delta G(1023\,\mathrm{K}) = -337\,\mathrm{kJ/mol}\end{gathered} \tag{4}$$

Jaroni [2] has investigated the dynamic interactions between molten aluminum and three reactive gases (Ar + 15% CO_2, Ar + 7% CO and Ar + 5% CH_4). The author establishes that there is a dependence on metal loss to treated gases, in the order of CO_2 > CO > CH_4. The definition of reaction mechanism is not given. The metal loss due to methane injection is described by reactions 5 and 6.

$$\begin{gathered}\mathrm{Al_{(l)}} + \frac{3}{4}\mathrm{CH_{4_{(g)}}} = \frac{1}{4}\mathrm{Al_4C_{3_{(s)}}} + \mathrm{H_{2_{(g)}}} \\ \Delta G(1023\,\mathrm{K}) = -59\,\mathrm{kJ/mol}\end{gathered} \tag{5}$$

$$\frac{3}{4}CH_{4(g)} = \frac{3}{4}C_{(s)} + \frac{3}{2}H_{2(g)} \quad \Delta G(1023\,K) = -17\,kJ/mol \tag{6}$$

Non-catalytic thermal decomposition of methane requires high temperature (>1000 K) due to the endothermic process. However, aluminum behaves as catalyst and favors the complete decomposition at lower temperatures [12, 13]. The same considerations apply to butane which decomposes to methane and propene.

Thermochemical Modelling

FactSage [9] is used for preliminary thermochemical modelling of the melting experiments to provide an overview of the possible reactions and their products. It is taken into account in all the representations shown in this chapter that the calculations are always based on reaction equilibrium. The equilibrium phases, which represent the system with the lowest total free enthalpy as a function of predetermined variables is based on steady state conditions. The temperature is set to 1023 K while the pressure of the melt and the added gas are set to 10^5 Pa. The high metal volume used in the calculations has the consequence that the gases CO_2, CO, O_2, C_4H_{10} and CH_4 are completely converted into solid reaction products except for H_2 and inert Ar. In Fig. 2 an example for a typical calculation done is presented. In this calculation 1 kg of Al melt reacts with a variable mole number of Ar + 5% CO_2. The main products are Al_2O_3 and Al_4C_3. In the case of C_4H_{10} and CH_4, the reaction products are Al_4C_3 and H_2.

In Fig. 3 the specific metal losses resulting from FactSage modelling are presented in a bar chart diagram. The diagram shows the simulated aluminum losses depending on injected gas mixtures. The calculations reveal the aluminum losses for circa 37 mol aluminum by addition of 3 mol gas. From the calculations, butane (C_4H_{10}) has the highest influence on aluminum loss related to the formation of aluminum carbides and hydrogen. The metal loss caused by butane is three time higher than methane (CH_4) due to the stoichiometric factor of carbon. Oxidative gases such as CO_2, CO and O_2 show less impact on dross formation. The metal losses by CO and CO_2 can be explained by the formation of Al_2O_3 and Al_4C_3.

Experiments

Experimental Procedure

Experiments were performed with pure aluminum (analyzed as 99.94 wt%) in an opened induction furnace. The following scheme (Fig. 4) shows the experimental setup.

A water-cooled copper induction coil, provided by medium frequency power, was installed into a furnace vessel. For melting, an alumina crucible (dimension: d = 95 mm, h = 105 mm) with a volume of 0.75 mm was used. The metal amount charged of all experiments was 1 kg. The reactive gas mixtures were injected through an alumina tube with a diameter of 40 mm into a 750 °C melt. Following gas mixtures were used: Ar + 5% O_2, Ar + 5% CO_2, Ar + 5% CO, Ar + 5% C_4H_{10} (butane), Ar + 5% CH_4 (methane). To realize an oxygen free atmosphere above the melt surface, an exhaust hood, which was continuously

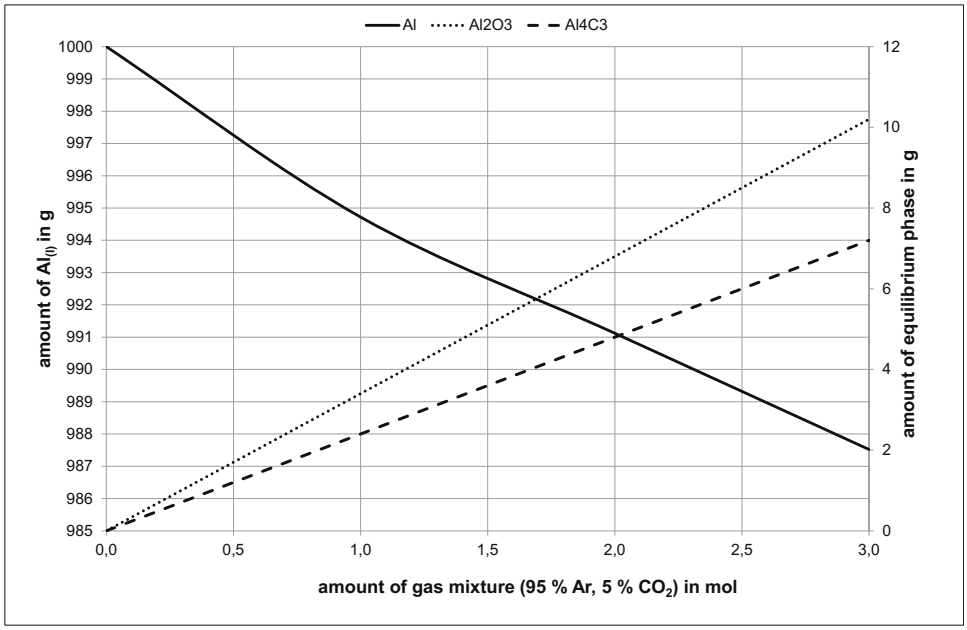

Fig. 2 FactSage modelled equilibrium for the reaction of 1 kg $Al_{(l)}$ + <a> Ar +5% $CO_{2(g)}$ with <a> up to 3 mol [9]

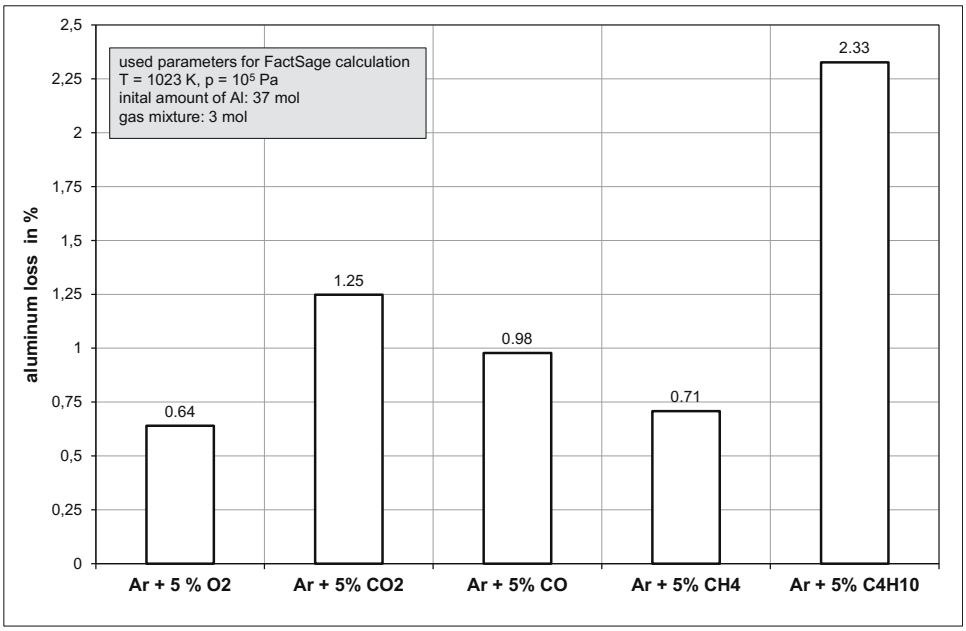

Fig. 3 Calculated aluminum loss in relation of injected gas mixture by FactSage [9]

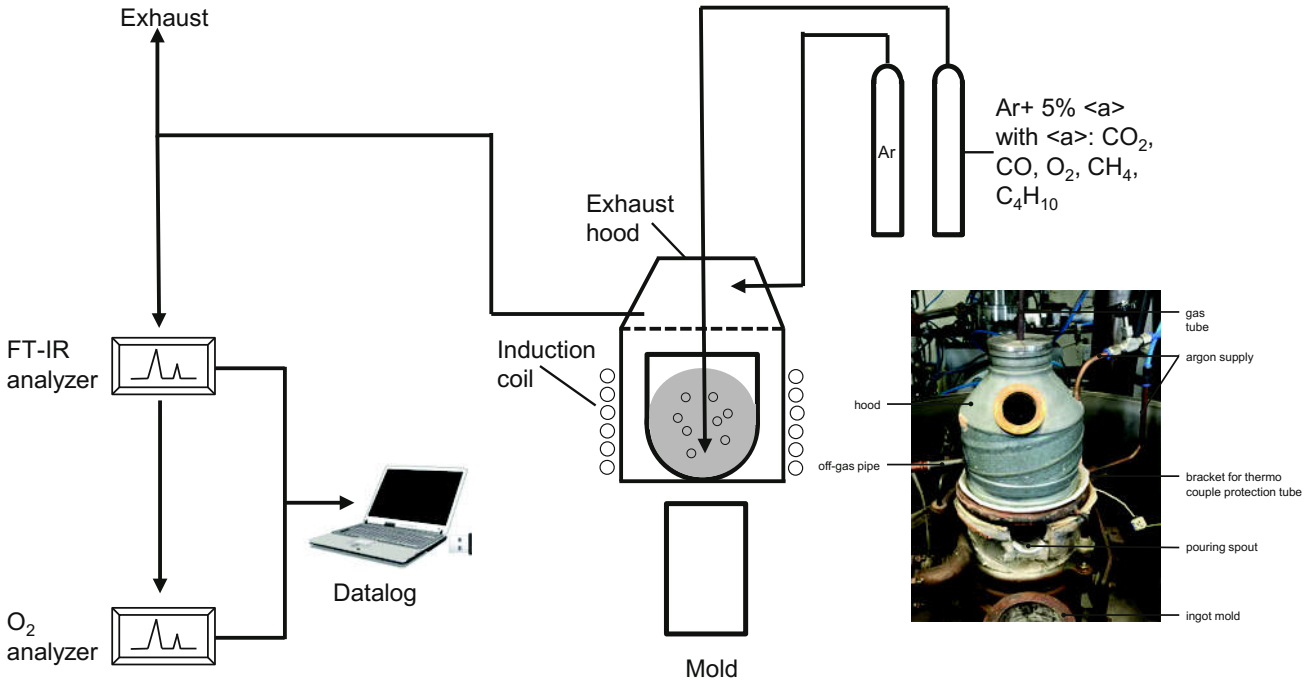

Fig. 4 Experimental setup with gas analyzing system and reaction chamber

flushed with protective argon (10 l/min), was positioned at the top of the coil. Gaseous reaction products were collected under the hood and supplied to an online gas measurement system. 15 tests were conducted, 3 per each injected gas to reach more reliability of the results. Before gas injection has been started, the tube was positioned 20 mm above melt surface for 10–20 min to record an initial value. Subsequently, the tube was immersed 40 mm into melt and such the gas injection started. During gas purging formed dross was skimmed three times (every 20 min) to achieve a refreshed melt surface, the solid product was cooled down under argon and weight. After 60 min the gas injection was stopped and molten aluminum was cast into a cylindrical mold under ambient atmosphere.

Experimental Results

In Fig. 5 the gross and net metal losses are presented, calculated by Eqs. 7 and 8. The gross metal losses increase in the series of $Ar < O_2 < C_4H_{10} < CH_4 < CO_2 < CO$, as a consequence of skimming procedure, the amount of dross is very high. To separate the metallic part from the nonmetallic components, a subsequent re-melting step under over-stoichiometric salt flux (55% NaCl, 45% KCl and 3% CaF_2) was performed.

$$\text{gross metal loss}\,\% = \frac{m_{cast}}{m_{initial}} \tag{7}$$

$$\text{net metal loss}\,\% = \frac{m_{cast} + m_{\text{metal recovery from dross}}}{m_{initial}} \tag{8}$$

The metal content of dross varies between 73 and 98% due to dross handling and stripping. Another reason can be established by metal entrapment in the dross structure which solidified and hinders the aluminum coalescence.

The net metal loss increases in the order of $Ar < O_2 < CH_4 < C_4H_{10}$, $CO < CO_2$. The greatest impact on metal loss can be attributed to CO_2, 17 times more than O_2, which was not expected on the first view. A significant difference between CO, C_4H_{10} and CH_4 cannot be determined. The moderate effect of O_2 on oxide formation may be attributed to formation of a direct formed protective oxide layer on the gas bubble surface.

During the experiments, gas analysis was measured continuously to verify the reaction potential of injected gases. Figure 6 shows the concentration profile of CO_2 consumed in the process.

At the beginning of the first 5 min, the CO_2-concentration decreases dramatically to 2000 ppm below start value and achieve a stable value of 2700 ppm below start after 15 min. After 30 min the gas purging is stopped, formed dross is skimmed, cooled down in argon atmosphere and gas purging starts again. The concentration difference due to consumed CO_2 is again around 2500 ppm. At the same time, a slight increase of CO concentration is measuring in off-gas. It is assumed that aluminum reacts with CO_2 under formation of CO and Al_2O_3 as indicated by Eq. 1. A further reaction lead to a decrease in CO concentration when CO_2 reaches its minimum. It is assumed, that CO reacts further with Al to Al_2O_3 and C, see reaction 2.

Before the dross is remelted under salt some samples are taken to analyze the initial dross composition. The total carbon concentration in dross as well as in metal has been analyzed by the total combustion method with Eltra CS 2000. This analysis method cannot distinguish between different carbon structures like elemental carbon or aluminum carbide. As Fig. 7 shows, the highest carbon content in dross is generated by injection of CO_2, following by CO, C_4H_{10} and CH_4. A two-step reaction from CO_2 to C is likely. The gas purging of CO is also leading to the formation of carbon. A significant difference in carbon content between methane and butane cannot be detected. A partial amount of carbon remains in metal and cannot float up to the metal/oxide surface due to the dynamic melt flow condition. Therefore, a comparison of the carbon content in metal related to the injected gas components is not useful.

Figure 8 shows a typical EDX analysis picture of a dross sample generated by CO_2 treatment, taken from the two marked areas in the macroscopic picture on the upper left.

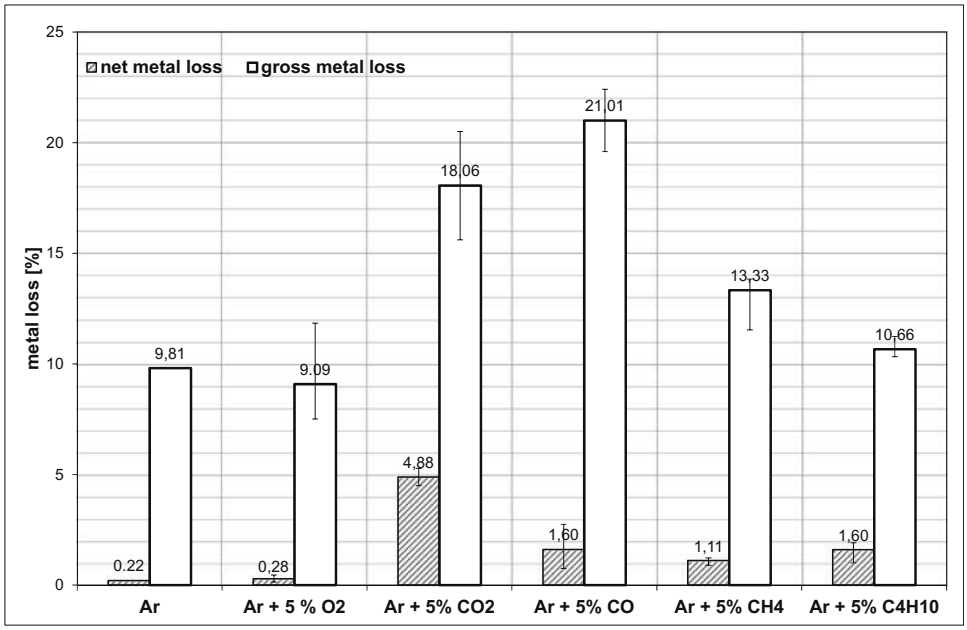

Fig. 5 Gross metal losses (ratio of casted ingot/metal input) and net metal losses (ratio of casted ingot + metallic drops in dross/metal input) generated by 3 mol of gas mixture injected in molten aluminum at 1023 K

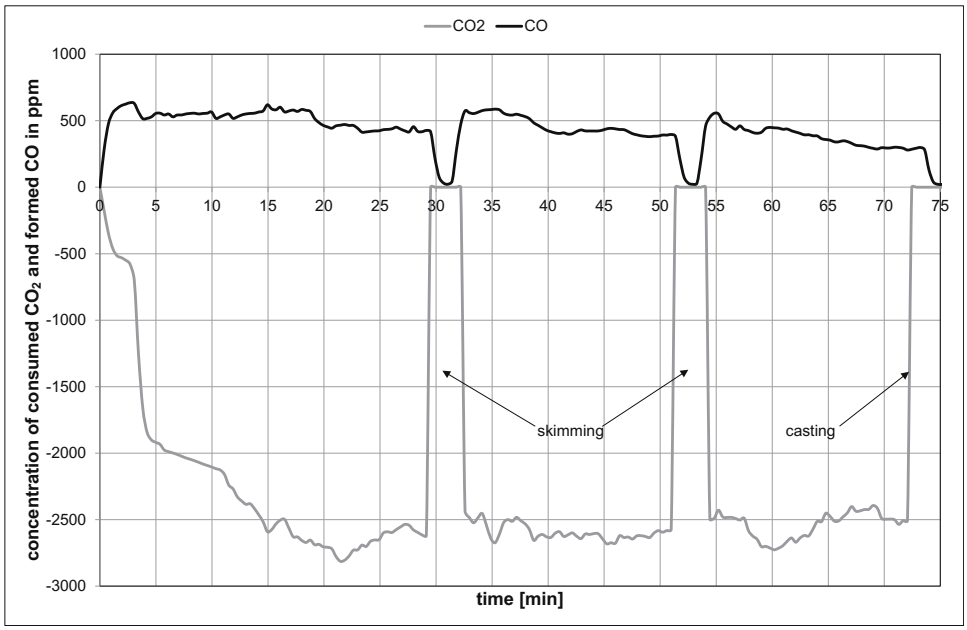

Fig. 6 Concentration profile of CO_2 (difference to initial value) and formed CO in argon atmosphere during CO_2 injection in molten aluminum (T = 1023 K)

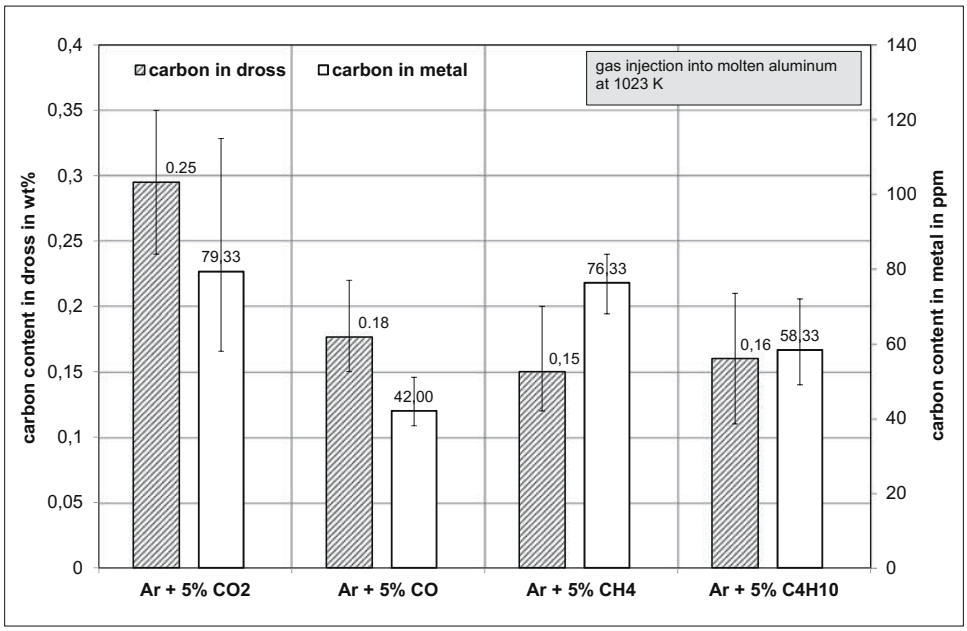

Fig. 7 Total carbon concentration in dross and metal regarding to injected gas component

The dross was mostly covered with fine black particles, easy identified as elemental carbon. The silver-grey film is not dense, reveals cracks and can be determined as a compound of Al and O.

The dross structures analysis is performed by XRD spectroscopy. Main dross phases for carbon containing components are aluminum oxide presented as γ-structure, graphite and metallic aluminum. A minor content of α-Al_2O_3 was measured as well. It may not be excluded that oxidation occurs when methane or butane are injected into melt according to a low oxygen concentration. Analysis of dross structure by oxygen injection has been proven metallic aluminum and γ-phase. XRD analyses have not proven carbide phases. One reason could be the limit detection for minor components as well as the subsequent re-oxidation due to low stability.

Discussion

Aluminum oxidation by O_2, CO_2 and CO

Aluminum oxidation occurs in the presence of all three oxidative gas components. However, oxide formation

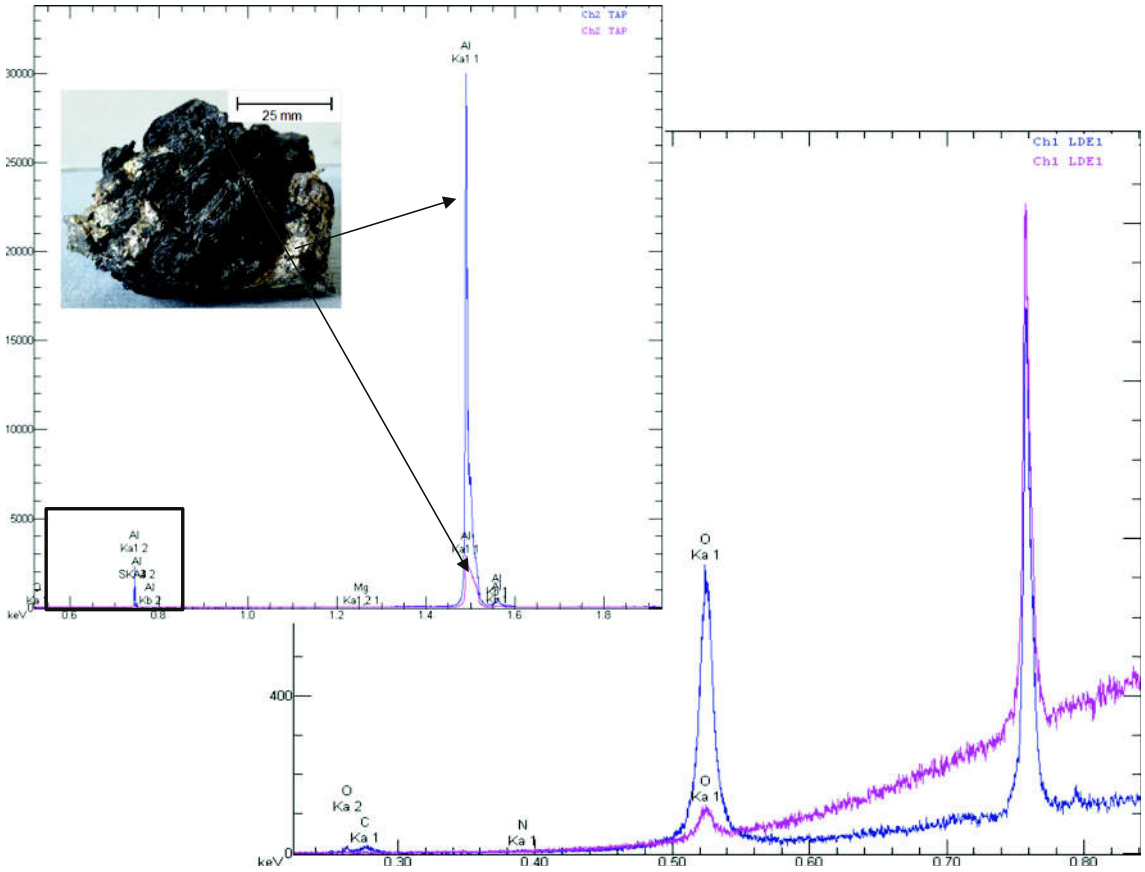

Fig. 8 EDX analysis of dross generated by CO_2 gas treatment

differs in their chemical reaction mechanism. In the presence of oxygen, a thin oxide layer of the crystalline γ-phase is directly formed on the bubble surface. As a result of this protective and dense layer, further oxidation is strongly reduced. Due to the short residence time of the gas bubble in the liquid metal, the phase transformation from γ to α does not take place. Breakaway oxidation and therefore a pronounced increase in oxidation rate is avoided.

The more complex aluminum oxidation by carbon dioxide contact is summarized in Fig. 9. In the first reaction step carbon dioxide is reduced by aluminum to carbon monoxide and Al_2O_3. In a second step CO reacts with the metal to C and Al_2O_3. The crystal structure of carbon is identified as graphite. Nevertheless, a low concentration of carbon monoxide in the off-gas is measured and a part of CO_2 leaves the melt without reaction. The formation and stability of aluminum carbide is not favorable in the presence of CO_2 according to the re-oxidation of carbon, as shown in Eq. 4. Consequently besides the formation of graphite, γ-Al_2O_3 is identified as main oxide phase in dross. A minor part is detected as α-Al_2O_3.

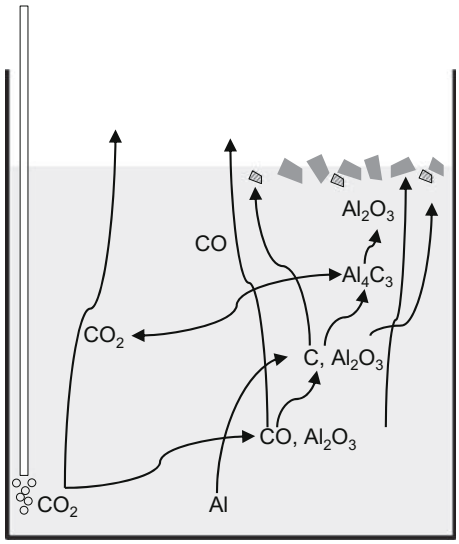

Fig. 9 Schematic drawing of reaction mechanism of liquid Al and CO_2

The injection of carbon monoxide leads to the formation of aluminum oxide and graphite as well as carbon dioxide but with less aluminum losses.

Aluminum interaction with CH_4 und C_4H_{10}

Liquid aluminum favors the thermal decomposition of hydrocarbons. As the off-gas measurement results show, methane and butane were consumed in the gas purging process. In the case of butane, the two gases methane and propene are identified as gaseous decomposition products. Butane as well as methane decompose to C and H_2 and such graphite can be identified in dross. The detected metal losses can be attributed to the low oxygen concentration in the furnace atmosphere due to the experimental set-up and procedure.

Summary

If the de-coating process of UBC bales is not completed in a reverberatory multi-chamber furnace, gasification will continue while the scrap is submerged into the melt. Subsequently, undesirable gas-melt reactions cause an increase of dross formation and a decrease of metal recovery. The aim of this work was to identify the reaction mechanisms between typical pyrolysis gas components and liquid aluminum. For experimental validation argon based gas mixtures with 5% of reactive gas components such as CO_2, CO, CH_4, C_4H_{10} and additional O_2 were injected through a lance into 99.9 wt% liquid aluminum at 1023 K.

Based on the results of loss calculations, the impact on dross formation increases in the order of O_2, CH_4, C_4H_{10}, CO, CO_2. Besides remelting measurements, off-gas analysis as well as structural dross analysis were conducted with regard to the postulated reaction mechanisms. Aluminum losses occurred by CO_2 can be explained by two step reactions: firstly, carbon dioxide is reduced by aluminum to carbon monoxide which reacts in a second step to solid carbon. The direct injection of carbon monoxide leads consequently to carbon and aluminum oxide formation. In the case of oxygen injection a thin protective oxide film is immediately formed on the bubble surface and hinders further reactions between melt and trapped oxygen.

Based on literature studies and experimental work, liquid aluminum acts as catalyzer for thermal decomposition of hydrocarbons to form graphite and hydrogen. Further reaction to aluminum carbide is not excluded but it could not be identified in this work. Due to the short time period of rising gas bubbles, butane is partly decomposed to methane and propene.

An important aspect for recycling aluminum scrap in an oxy fuel combustion furnace is the effect of humidity on dross formation. Therefore it is necessary to further verify the reactivity of water saturated gas mixtures in contact with molten aluminum. Also the effect of alloying elements on dross formation must be investigated in the ongoing research project. According to typical compositions the impact of magnesium on reactions steps will be in detail analyzed.

Acknowledgements The research leading to these results has been carried out within the framework of the AMAP (Advanced Metals And Processes) research cluster at RWTH Aachen University, Germany. The authors like to thank Aleris Rolled Products Germany GmbH, Constellium, Hydro Aluminium Rolled Products GmbH and Trimet Aluminium SE for financial support. Furthermore, the Master Thesis of student Felix Pleuger is gratefully acknowledged.

References

1. J. Steglich et al., Pre-treatment of beverage can scrap to increase recycling efficiency. Eur. Aluminium Congr. 2015, Düsseldorf (2015)
2. B. Jaroni, Einfluss von organischen Komponenten auf das Aluminiumrecycling. Ph.D. thesis, RWTH University, ISBN: 3844026339 (2014)
3. A. Kvithyls et al., Gases evolved during de-coating of aluminium scrap in inert and oxidizing atmospheres. Light Met. 1091–1095 (2003)
4. S. Levchik, E. Weil, Thermal decomposition, combustion and flame—retardancy of epoxy resins—a review of the recent literature. Polym. Int. **53**, 1901–1929 (2004)
5. M. Wang et al., Study on de-coating used beverage cans with thick sulfuric acid for recycle. Energy Convers. Manag. **48**(3), 819–825 (2007)
6. K. Brenzinsky, M. Pecullan, I. Glassmann, Pyrolysis and oxidation of phenol. J. Phys. Chem. A **102**, 8614–8619 (1998)
7. W. Thiele, Die oxydation von aluminium- und aluminium legierungs-schmelzen. Aluminium **38**(12), 707–715 (1962)
8. E. Bergsmark, C. Simensen, P. Kofstad, The oxidation of molten aluminium. Mater. Sci. Eng. A **120**, 91–95 (1989)
9. S. Bonner, Oxidation of commercial purity aluminum melts: an experimental study. Light Met. 993–997 (2013)
10. G. Wigthman, D. Fray, The dynamic oxidation of aluminum and its alloy. Metall. Trans. **14b**, 625–631 (1983)
11. FactSage 6.4 2013, Thermfact
12. C. Thomas et al., Catalytic effect of metals on paraffin hydrocarbons. Ind. Eng. Chem. **31**(9), 1090–1098 (1939)
13. M. Serban et al., Hydrogen production by direct contact pyrolysis of natural gas. Energy Fuels **17**(3), 705–713 (2003)